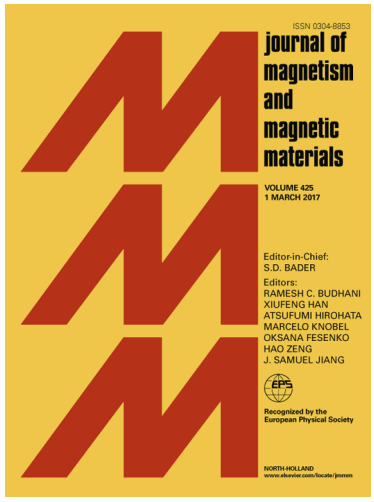

Research articles

The anisotropic tunneling behavior of spin transport in graphene-based magnetic tunneling junction

Mengchun Pan, Peisen Li, Weicheng Qiu, Jianqiang Zhao, Junping Peng, Jiafei Hu, Jinghua Hu, Wugang Tian, Yueguo Hu, Dixiang Chen, Xuezhong Wu, Zhongjie Xu, Xuefeng Yuan

PII: S0304-8853(17)32954-2
DOI: https://doi.org/10.1016/j.jmmm.2018.01.016
Reference: MAGMA 63594

To appear in: *Journal of Magnetism and Magnetic Materials*

Received Date: 16 September 2017
Revised Date: 16 December 2017
Accepted Date: 6 January 2018

Please cite this article as: M. Pan, P. Li, W. Qiu, J. Zhao, J. Peng, J. Hu, J. Hu, W. Tian, Y. Hu, D. Chen, X. Wu, Z. Xu, X. Yuan, The anisotropic tunneling behavior of spin transport in graphene-based magnetic tunneling junction, *Journal of Magnetism and Magnetic Materials* (2018), doi: https://doi.org/10.1016/j.jmmm.2018.01.016

The anisotropic tunneling behavior of spin transport in graphene-based magnetic tunneling junction

Mengchun Pan[1], Peisen Li[1], Weicheng Qiu[1], Jianqiang Zhao[1], Junping Peng[1], Jiafei Hu[1], Jinghua Hu[1], Wugang Tian[1*], Yueguo Hu[1], Dixiang Chen[1], Xuezhong Wu[1], Zhongjie Xu[2] and Xuefeng Yuan[3]*

[1]College of Mechatronic Engineering and Automation, National University of Defense Technology, Changsha, Hunan, China, 410073

[2]College of Optoelectronic Science and Engineering, National University of Defense Technology, Changsha, Hunan, China, 410073

[3]National Supercomputer Center in Guangzhou, Guangzhou, China, 510000

*Corresponding author: e-mail lips13@163.com

**Corresponding author: e-mail twg_1978@163.com

ABSTRACT

Due to the theoretical prediction of large tunneling magnetoresistance (TMR), graphene-based magnetic tunneling junction (MTJ) has become an important branch of high-performance spintronics device. In this paper, the non-collinear spin filtering and transport properties of MTJ with the Ni/tri-layer graphene/Ni structure were studied in detail by utilizing the non-equilibrium Green's formalism combined with spin polarized density functional theory. The band structure of Ni-C bonding interface shows that Ni-C atomic hybridization facilitates the electronic structure consistency of graphene and nickel, which results in a perfect spin filtering effect for tri-layer graphene-based MTJ. Furthermore, our theoretical results show that the value of tunneling resistance changes with the relative magnetization angle of two

ferromagnetic layers, displaying the anisotropic tunneling behavior of graphene-based MTJ. This originates from the resonant conduction states which are strongly adjusted by the relative magnetization angles. In addition, the perfect spin filtering effect is demonstrated by fitting the anisotropic conductance with the Julliere's model. Our work may serve as guidance for researches and applications of graphene-based spintronics device.

Key words: graphene, magnetic tunneling junction, spintronics device, non-collinear, anisotropy

The magnetic tunneling junction (MTJ) consists of an insulating barrier which is sandwiched by two ferromagnetic metal (FM) electrodes with variable magnetization direction. The tunneling resistance of MTJ is closely related to the relative magnetization direction of FM electrodes and can be controlled by external applied magnetic fields. As a kind of elemental spintronics device, MTJs have a wide range of applications, such as magnetic random access memories, read heads and magnetic sensors.[1-4] Generally, the spin filtering effect at the ferromagnet/insulator interface is one of the key factors to achieve large tunneling magnetoresistance (TMR) and spin injection efficiency of MTJ.[2,5,6] So far, AlO_x and MgO have been widely used as the insulating barriers. However, the unavoidable pinholes in the thin oxidation-barriers and the oxidation defects of adjacent FM films jointly cause the non-uniform of the barrier/ferromagnet (Fe, Co and Ni) interfaces, which extremely limits the spin filtering and TMR in MTJ.[7,8] Hence, exploring potential materials as the barrier to achieve larger TMR and higher spin filtering has become a hot research point in spintronics.[9] Nowadays, graphene as a kind of important two-dimensional material has triggered a wave of research interest in spintronics device for the following reasons.

- The linear dispersion near Fermi level and massless electrons make graphene a promising material for application in microelectronic devices, such as field-effect transistors (FET), photoelectric device and quantum Hall device, etc.[10-13]

- Graphene has been paid more attention to on the spin degree due to its unique magnetism and magnetoelectronics properties, such as the local magnetic moment induced by defect,[14-16] half-metallic properties performed in graphene nanoribbons,[17] and spin electrons injected into the graphene channel.[18-20] Meanwhile, the weak spin-orbit interaction and hyperfine coupling result in a long relaxation time and a large relaxation length of the spin electron in graphene, which demonstrates that graphene is a good choice for the fabrication of high-performance spin electron transport devices.

- Due to its atomic thickness, favorable chemistry stability and well lattice matching with FM electrode Ni (111) and Co (0001), graphene can be used as an ideal barrier layer of MTJ for efficient spin filtering. This has been demonstrated by the previous theoretical researches, where the results show that the graphene-based MTJs emerge nearly 100% spin filtering and 100 times larger magnetoresistance ratio compared with that of MgO-based MTJs.[7,21]

Up to date, theoretical works have provided insightful contributions to the physics of graphene-based MTJ, and show that the atomic hybridization between FM electrodes (Co and Ni) and graphene leads to the spin-dependent shifting and opening of graphene's Dirac points (DP), which results in a perfect spin filtering effect. However, current theoretical research on graphene-based MTJs focused on the spin-polarized electron transport for parallel (A) or antiparallel (AP) orientation of the FM electrode magnetizations and lacked that for the anisotropy effect of spin transport in graphene-based MTJ. It is well known that the anisotropy effect is very

informative to understand the nature of spin electron transport and facilitate the application in the magnetic field sensors.[22] For example, Chen *et al* performed the angular dependence of exchange bias to verify the correctness of the theoretical model.[23] Fratini *et al* also reported the anisotropic intrinsic spin relaxation introduced by the flexural distortions in graphene.[24] Hence, it is thus clear that the anisotropy effect of magnetoresistance is one of the intriguing features.

For this reason, the spin-dependent transport properties with different magnetization orientations have been studied by *ab* initio Atomistix ToolKit (ATK) software with density functional theory (DFT) and the non-equilibrium Green's function method in this paper.[25] The electronic structure around graphene/FM interfaces and the interaction between graphene and FM electrode have been analyzed by the spin-dependent band structure of Ni/graphene (Gr)/Ni super-lattice cell. The strong Ni-C atomic orbital hybridization between FM electrodes and graphene contributes to the large spin filtering efficiency in graphene-based MTJ. More importantly, the spin-dependent transmission spectrum and position-dependent local density of state (LDOS) of MTJ under different magnetization originations have been further studied here by introducing the non-collinear magnetization calculation method. In this method, we got configuration at some angle theta firstly, and then performed self-consistent non-collinear DFT calculations to obtain true Hamiltonian at angle theta between the magnetizations. The results show that resonant conduction states closely depend on the FM electrodes magnetization originations, which strongly affects the tunneling transmission properties of spin electrons. In addition, the perfect spin filtering effect is demonstrated by fitting the anisotropic conductor with the Julliere's model. These results are helpful for further understanding the spin transport in graphene-based MTJ, and the methods used in this paper give a formwork for

investigating the anisotropy effect of the spintronics.

The FM/Gr/FM MTJ nanostructure was constructed as illustrated in Fig. 1(a), where Ni (111) (green) was used as two FM electrodes due to its little lattice mismatch with graphene (1.3%).[21] A tri-layer graphene (gray) sandwiched between two Ni electrodes was chosen as the barrier to get appropriate TMR and junction resistance. The left and the right electrodes of the device were infinitely periodic along the vertical direction of *z*-axis and both electrodes were subjected to applied magnetic fields (blue arrows), which results in magnetization on both electrodes (M_L and M_R). To clearly express our perspective, the simplified P and AP configuration are used to describe parallel and antiparallel magnetization orientation of two FM electrodes, respectively. The *AC* structure, in which the top-site C atom is located above the Ni atom while the hollow-site C atom is located above a third layer Ni site, was chosen because it has the minimum total energy as previously reported.[21] The lattice constant of graphene was increased to 2.49 Å, which is consistent with that of Ni (111) surface. The electrodes were set to four layers with the thickness of about 8.1 Å. To obtain the properties of the band structure, a super-lattice box of Ni/Gr/Ni nanostructure was chosen. The vacuum layer on both sides of Ni layers was set to 9 Å. The Brillouin zone sampled with 11×11×1 k-point grids was set for the band structure calculations. The total energy calculated to the interfacial structures was optimized by minimizing the energy within the local spin density approximation (LSDA) of DFT.

After geometry optimization, the spin-dependent transmission properties of two-probe geometry (See Fig. 1) were simulated using DFT combined with the non-equilibrium Green's function (NEGF) method. The single ζ-polarized (SZP) basis on C atoms and double ζ-polarized (DZP) basis on Ni atoms were chosen for atomic orbital basis sets. Troullier-Martin type pseudo-potentials were used. The LSDA with

PZ approximation was employed for the exchange-correlation potential. In the simulation, the Brillouin zone was sampled by 12×12×151 k-point grids, and LDOS, as well as transport calculations, were determined on a real-space grid with a mesh cutoff energy of 150 Ry.

The spin-dependent bands of Ni/Gr/Ni super-lattice cell under parallel magnetization orientation were firstly studied to investigate the electronic structure and the interaction of graphene with FM electrode in the interface. The results are shown in Fig. 1(b, c) for the majority spin (α-spin) and minority spin (β-spin), respectively. For the sake of clarity, the simplified α-spin and β-spin are used to describe majority and minority spin states defined as the left Ni FM electrode magnetization direction definition. It can be firstly seen that the Dirac point of graphene shifts down about 0.6 eV due to the charge transfer from C to Ni atoms for the α-spin and β-spin, which is consistent well with the work function difference between the Ni (5.2 eV) and graphene (4.6 eV).[26] Secondly, the graphene Dirac band opens a gap about 0.3 eV at the K point (See Fig. 1(b)) for α-spin, but has no influence on the bandgap for β-spin. At the same time, the natural linear dispersion relation of graphene is destroyed, meaning a non-massless nature of the graphene electron. Thirdly, the two parabolic bands of tri-layer graphene shift up about 0.2 eV and 0.6 eV for α-spin and β-spin, respectively. All these distributions of band structures after coupling with Ni electrodes exhibit the obvious spin-dependent characteristics, meaning a strong chemisorption of graphene with Ni electrode as previously studied.[21] Meanwhile, this strong chemisorption means a strong hybridization between the orbits of graphene and the Ni electrode, leading to the formation of a spin-dependent interface and a significant shift of the graphene bands with respect to the Fermi level. It is crucial to note that the strong orbital hybridization

between graphene and Ni attributed mainly to the coupling of C atom p_z-orbit and Ni atom d_z-orbit. Interestingly, it appears that the coupling of carbon band and nickel band occurs mainly at an energy level of -0.5 eV below Fermi level for α-spin, while from -0.3 eV below Fermi level to 0.3 eV above Fermi level for β-spin, respectively. This is due to the β-spin bands hybridize with both π and π* bands of graphene, and α-spin bands mainly hybridize with π band. As a result, the hybridized π and π* bands of graphene will play different roles in the spin electron transport, which is distinguished from the pure graphene.

As discussed above, the Ni-C atomic hybridization would promote the electronic structure consistency of graphene and nickel, which may result in a perfect spin filtering effect for tri-layer graphene-based MTJ. This was confirmed by the simulation of transmission spectrum under P and AP configurations, respectively. Figure 1(d) shows the spin-dependent transmission spectrum of MTJ under P configuration. Since α-spin bands mainly hybridized with π bands of graphene at an energy level of about -0.5 eV, the transmission spectrum under P configuration shows a weak peak at about -0.5 eV below the Fermi level. By contrast, the transmission spectrum of β-spin under P configuration shows a sharp peak around the Fermi level ranged from -0.3 eV to 0.3 eV, which is consistent with the band structure shown in Fig. 1(c). This transmission sharp peak corresponds to both π and π* bands of graphene hybridized with the β-spin bands, which results that both conduction electrons and valence electrons can contribute to the transmission coefficients. Additionally, there are large density of states (DOS) at Fermi surface for β-spin electron around the interface between graphene and Ni electrode after the Ni-C hybridization. Hence, when graphene's DOS have coupled to available states in two Ni electrodes, the β-spin electron could pass unobstructed through the graphene

barrier as a resonance tunneling way. On the other hand, the transmission behaviors under AP configuration for α-spin and β-spin electrons are both very weak, as shown in Fig. 1(e). This is mainly due to the significant reduction of total transport electrons, where the electrons of α-spin bands (β-spin bands) in one electrode transmit into the empty states of β-spin bands (α-spin bands) in another electrode under AP configuration.

Note that the spin-dependent transmission spectrum is strongly influenced by the configurations of the FM electrodes, indicating it will be meaningful to study the anisotropic behaviors of the spin transport under different magnetization configurations. In this case, we investigated the anisotropic spin transport properties of graphene-based MTJ by using the non-collinear spin-resolved calculation method. In the simulation, the magnetization direction of M_L is set along the z-axis direction of the devices, while the magnetization direction of M_R is deviated an angle θ from z-axis, as shown in Fig. 2(a). The calculation results of θ-dependent transmission spectrum are shown in Fig. 2(b) and Fig. 2(c) for α-spin and β-spin, respectively. We can see that the transmission peak below the Fermi level of α-spin depresses as the angle increases, and the transmission peak near the Fermi energy level of β-spin electron decreases with the increase of angle θ at the same time. Since that the transport current of the device is mainly contributed by the electron near the Fermi energy level, the conductance of β-spin electron is seriously impacted by the angle θ while the α-spin electron is not. This is further confirmed by the results of conductance dependence on angle θ, as shown in Fig. 3(a). It can be found that the conductance of β-spin electron decreases sharply with the angle θ, while the conductance of α-spin electron is almost independent on the magnetization directions.

To understand the spin filtering affected by the anisotropy, the spin filtering

coefficient η as a function of angle θ was obtained from the data of θ dependences of two spin conductance (G) (see Fig.3 (a)), where the spin filtering coefficient η was defined as $\eta = (G_\alpha - G_\beta)/(G_\alpha + G_\beta)$. As can be seen from Fig. 3(b), the spin filtering coefficient η decreases slowly with the increase of θ below 90°, whereas it decreases sharply with the increase of θ over 90°. The result of θ dependences of η demonstrates that the spin transport channel between graphene and FM electrodes could be tightly controlled by magnetization orientations.

On the other hand, the curve of the total conductance G_s varied with angle θ is shown in Fig. 3(c) marked with the circular dates, where $G_s = G_\alpha + G_\beta$. Based on the classical MTJ Julliere's model,[27] the anisotropic conductance G_s as a function of angle θ can be written as follows:

$$G_s(\theta) = G_s(0) \cdot (1 + P_1.P_2 \cos(\theta)) \quad (1)$$

Where P_i (i=1, 2) is the effective spin polarization of two FM electrodes and $G_s(0)$ is the conductance under P configuration. The extracted effective spin polarization ($P_1 = P_2 \approx 0.89$) is much larger than intrinsic spin polarization of Ni electrode, which demonstrates the high spin polarization effect of graphene-based MTJs stems from the efficient spin filtering at the Ni/Graphene interface. To study the effect of magnetization orientation on resistance value, the definition of angle-dependent magnetoresistance (MR) is different from the traditional tunneling magnetoresistance defined as $TMR = (G_P - G_{AP})/G_{AP}$, where $G_P = G_s(0)$ represents the device conductance under P configuration, and $G_{AP} = G_s(180)$ represents the device conductance under AP configuration. The MR as a function of angle θ is written as follows:

$$MR(\theta) = \left| \frac{G_s(\theta) - G_s(0)}{G_s(\theta) + G_s(0)} \right| \quad (2)$$

The MR value returns to zero when the device is under P configuration and reaches close to the limit 100% when it is under AP configuration. This definition takes a visualized way to describe the strength of the anisotropic tunneling effect. The curve of MR with angle θ has been extracted from the conductance data as shown in Fig. 3(d), which displays the characteristics of anisotropic tunneling behavior. Meanwhile, the theoretical results show that the value of MR linearly changes with the relative magnetization angle, which is expected to be applied in magnetic field direction measurement. Besides, these results also get rid of the anisotropy mainly from the spin tunneling.

It is also meaningful to research the different cases where the electrodes both are parallel to the junction plane. Hence, we also calculated the result of the case where the magnetization direction of one electrode is rotated from initial position while the other electrode is remain the same direction with the magnetization along the X direction, but both are parallel to the junction plane, according to the method of TAMR in MgO-MTJ.[28,29] The curve of G_s changed with angle θ is shown in Fig. 3(c) marked with the square dates. It is clear that the situation of in-plane case is similar with that of the first case (out-plane) in our MTJ structure. To obtain the compared effect of the FM magnetization on spin transport at in-plane and out-plane cases, we extracted the difference of G_s as the function of the angle:

$$\Delta(\theta) = \frac{(G_{s,Outplane}(\theta) - G_{S,Inplane}\theta))}{G_{s,Outplane}(180)} \tag{3}$$

The result is shown in the inset of the Fig. 3(c), which demonstrates a more larger MR in out-plane case caused by the tunnel anisotropic magnetoresistance (TAMR) effect It is noted that this TAMR effect in Ni/Gr/Ni junction is small compared with the MgO-MTJ,[28] one of the main reasons seems to be the weak spin-orbit coupling effect

of graphene.

Further insight into the microscopic mechanism behind the spin transport dependence on magnetization orientation in Ni/Gr/Ni junctions can be explained by examining the LDOS. The position-dependent LDOS for β-spin electrons is plotted in Fig. 4, where six angle values (θ = 0°, 60°, 90°, 120°, 150°, 180°) are chosen. Under P configuration (θ = 0°), a prominent resonant state in the central graphene region is located close to the Fermi level and couples well with the conduction states of both Ni electrodes (white and red regions), which is consistent with the report in the literature.[30] With the increase of angle θ, the position of resonant state starts to change dramatically. Part of the resonant state is enclosed by the fact that the conduction state remains unchanged in the left Ni electrode while follows rigidly the downward-moving conduction state in the right Ni electrode. As a result of this, the resonant state gets modified with the angle θ, thereby losing the coupling to one of the Ni electrodes. Thus, the electron transport is gradually suppressed with the increase of angle θ.

In summary, the mechanism for anisotropic tunneling MR of graphene-based MTJ was investigated in this letter. Theoretical analysis demonstrated that Ni-C hybridization may contribute to the perfect spin filtering transport in Ni/Gr/Ni sandwich structure. The transmission spectrum and spin-resolved LDOS at different magnetization orientation are analyzed in detail for the anisotropic tunneling behavior of the graphene-based MTJ. The resonant state modified by the magnetization orientation is possibly the main reasons that result in the meaningful anisotropic tunneling behavior. The work in this paper can provide a theoretical basis for anisotropic spin transport mechanism in graphene-based MTJs, as well as guidance for the application of graphene-based MTJs in future spintronics device.

ACKNOWLEDGEMENTS

This work is supported by National Science Foundation of China (Grants U1430105, 61671460, 51507178 and 11604384), Specialized Research Fund for the Doctoral Program of Higher Education (Grant 20124307120012), China Postdoctoral Science Foundation (Grant 2016M603000) and Research Project of National University of Defense Technology (Grant JC15-03-02).

References:

1 S. A. Wolf, D. D. Awschalom, R. A. Buhrman, J. M. Daughton, S. von Molnár, M. L. Roukes, A. Y. Chtchelkanova, and D. M. Treger, Science **294**, 1488 (2001).

2 X. Han, S. S. Ali, and S. Liang, Science China (Physics, Mechanics & Astronomy) **56**, 29 (2013).

3 A. D. Kent and D. C. Worledge, Nat. Nanotechnol. **10**, 187 (2015).

4 S. Cardoso, D. C. Leitao, L. Gameiro, F. Cardoso, R. Ferreira, E. Paz, and P. P. Freitas, Microsystem Technologies **20**, 793 (2014).

5 W. H. Butler, X. G. Zhang, T. C. Schulthess, and J. M. MacLaren, Phys. Rev. B **63**, 54416 (2001).

6 S. S. P. Parkin, C. Kaiser, A. Panchula, P. M. Rice, B. Hughes, M. Samant, and S. Yang, Nat. Mater. **3**, 862 (2004).

7 V. Karpan, G. Giovannetti, P. Khomyakov, M. Talanana, A. Starikov, M. Zwierzycki, J. van den Brink, G. Brocks, and P. Kelly, Phys. Rev. Lett. **99**, 176602 (2007).

8 M. Piquemal-Banci, R. Galceran, S. Caneva, M. B. Martin, R. S. Weatherup, P. R. Kidambi, K. Bouzehouane, S. Xavier, A. Anane, F. Petroff, et al, Appl. Phys. Lett. **108**, 102404 (2016).

9 W. Han, R. K. Kawakami, M. Gmitra, and J. Fabian, Nat. Nanotechnol. **9**, 794 (2014).

10 A. K. Geim and K. S. Novoselov, Nat. Mater. **6**, 183 (2007).

11 K. S. Novoselov, A. K. Geim, S. V. Morozov, D. Jiang, M. I. Katsnelson, I. V. Grigorieva, S. V. Dubonos, and A. A. Firsov, Nature **438**, 197 (2005).

12 K. S. Novoselov, A. K. Geim, S. V. Morozov, D. Jiang, Y. Zhang, S. V. Dubonos, I. V. Grigorieva, and A. A. Firsov, Science **306**, 666 (2004).

13 C. L. Kane and E. J. Mele, Phys. Rev. Lett. **95**, 226801 (2005).

14 B. Uchoa, V. Kotov, N. Peres, and A. Castro Neto, Phys. Rev. Lett. **101**, 026805 (2008).

15 S. Dutta and K. Wakabayashi, Sci. Rep. **5**, 11744 (2015).

16 R. R. Nair, M. Sepioni, I. Tsai, O. Lehtinen, J. Keinonen, A. V. Krasheninnikov, T. Thomson, A. K. Geim, and I. V. Grigorieva, Nat. Phys. **8**, 199 (2012).

17 Y. Son, M. L. Cohen, and S. G. Louie, Nature **444**, 347 (2006).

18 A. Dankert, M. V. Kamalakar, J. Bergsten, and S. P. Dash, Appl. Phys. Lett. **104**, 192403 (2014).

19 N. Tombros, C. Jozsa, M. Popinciuc, H. T. Jonkman, and B. J. van Wees, Nature **448**, 571 (2007).

20 M. V. Kamalakar, C. Groenveld, A. Dankert, and S. P. Dash, Nat. Commun. **6**, 6766 (2015).

21 V. M. Karpan, P. A. Khomyakov, A. A. Starikov, G. Giovannetti, M. Zwierzycki, M. Talanana, G. Brocks, J. van den Brink, and P. J. Kelly, Phys. Rev. B **78**, 195419 (2008).

22 M. Hell, S. Das, and M. R. Wegewijs, Phys. Rev. B **88**, 115435 (2013)

23 A. Chen, Y. Zhao, P. Li, X. Zhang, R. Peng, H. Huang, L. Zou, X. Zheng, S. Zhang, P. Miao, et al, Adv. Mater. **28**, 363 (2016).

24 S. Fratini, D. Gosálbezmartínez, P. M. Cámara, and J. Fernándezrossier, Phys. Rev. B **88**, 115426 (2012).

25 "Atomistix ToolKit version 2013." QuantumWise A/S (www.quantumwise.com).

26 K. Nagashio, T. Nishimura, K. Kita, and A. Toriumi, Appl. Phys. Lett. **97**, 143514 (2010).

27 M. Julliere, Phys. Lett. A **54**, 225 (1975).

28 M.N. Khan, J. Henk, and P. Bruno, J. Phys.: Condens. Matter **20**, 155208 (2008).

29 A. M. Abiague, and J. Fabian, Phys. Rev. B **79**, 155303 (2009).

30 K. K. Saha, A. Blom, K. S. Thygesen, and B. K. Nikolić, Phys. Rev. B **85**, 184426 (2012).

Figures caption

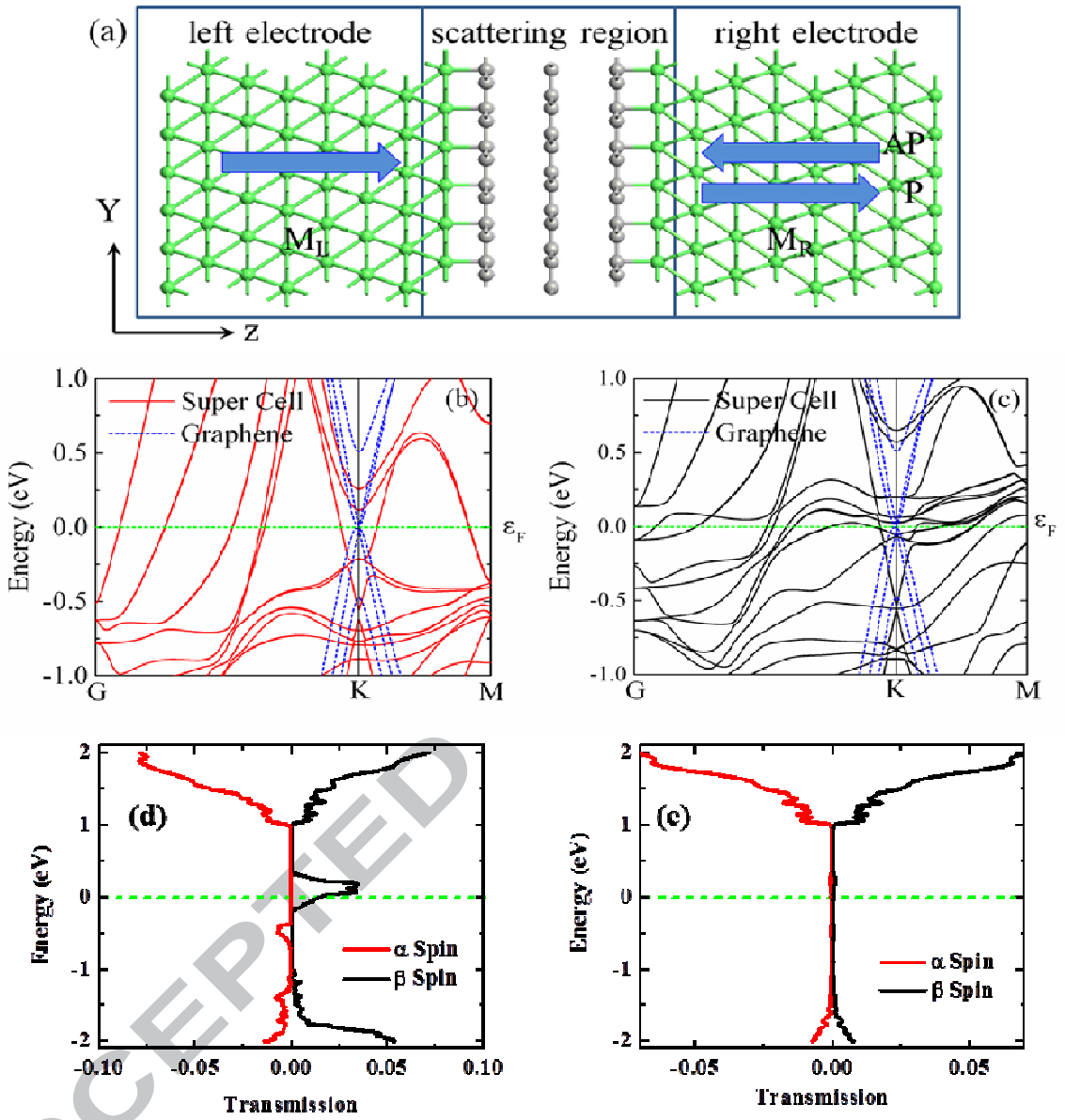

FIG. 1. (Color online) (**a**) Geometric structure of the graphene-based MTJ device with tri-layer graphene between two ferromagnetic Ni electrodes. The band structures of (**b**) α-spin and (**c**) β-spin of Ni/Gr/Ni super-lattice cell, respectively. The spin-dependent transmissions as a function of energy for the (**d**) P and (**e**) AP configuration, respectively. The Fermi level is shifted to 0 (the green dotted-line).

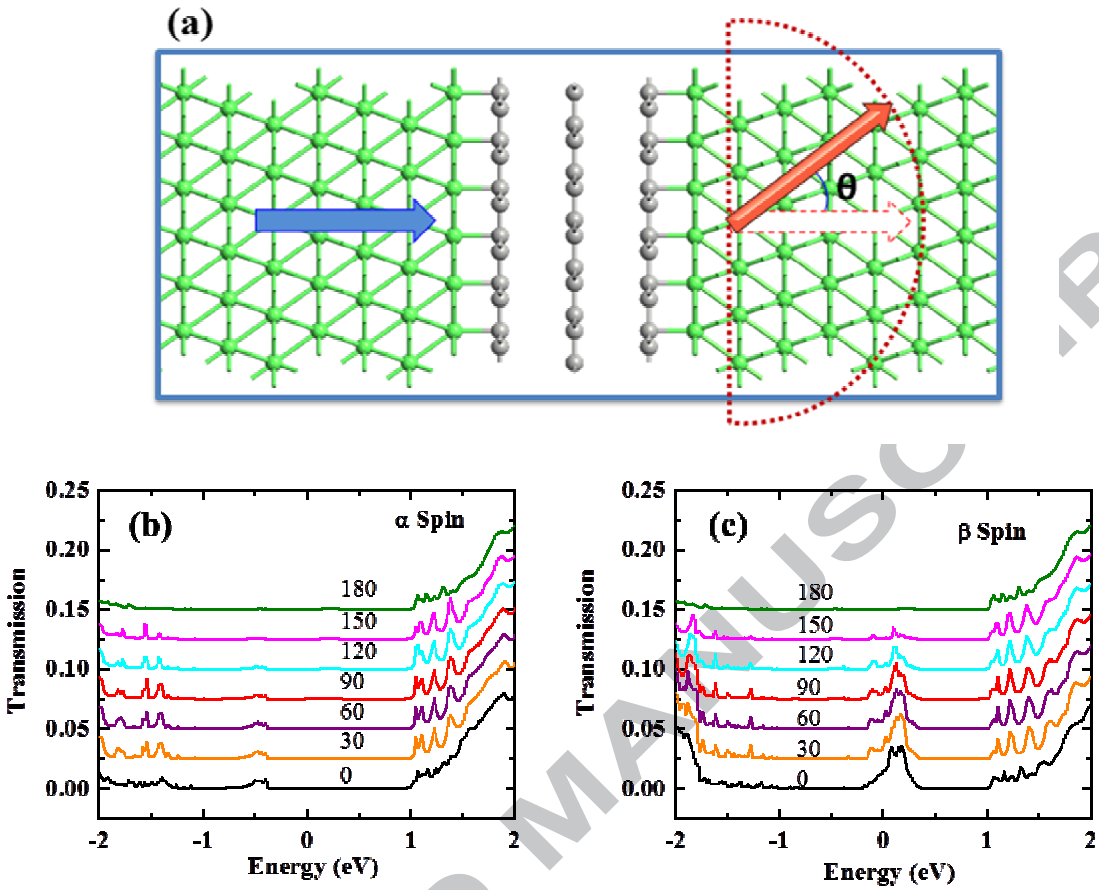

FIG. 2. (Color online) (**a**) The angle θ between the two magnetic directions of the layers. The transmission spectrums at different angles θ for (**b**) α-spin and (**c**) β-spin electronics, respectively. (the curves were offset for eye guide)

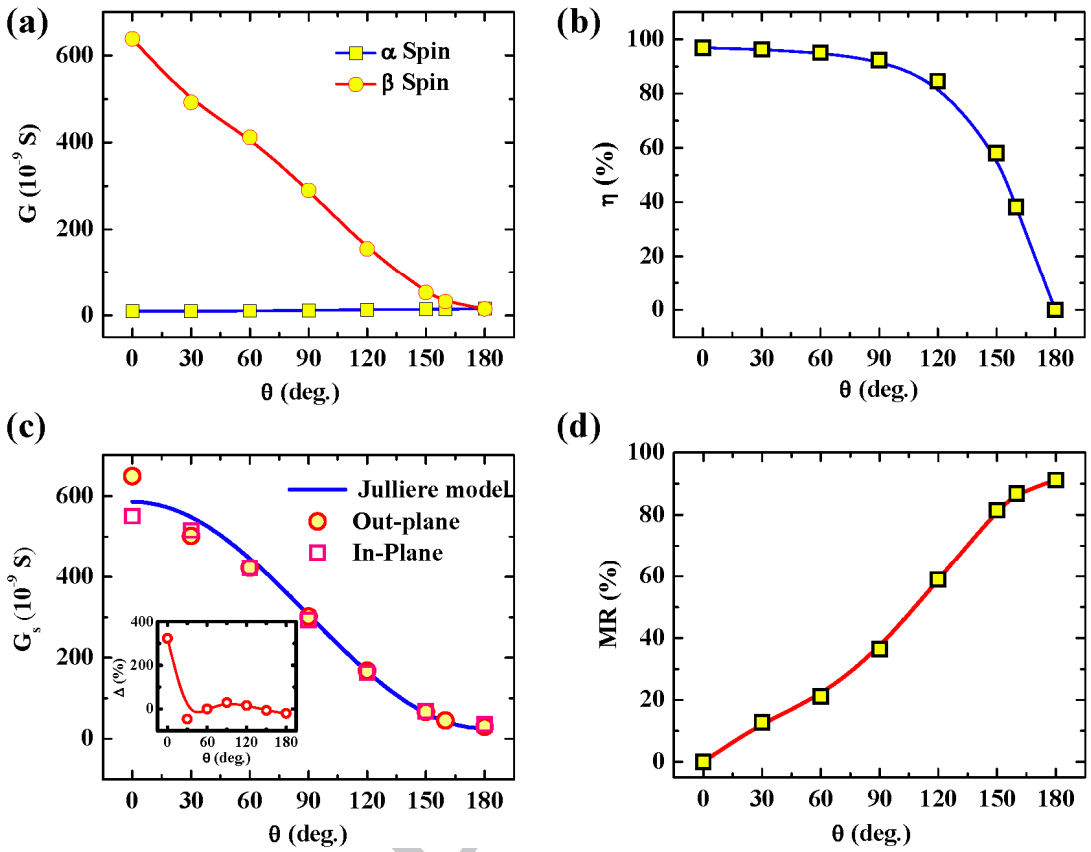

FIG. 3. (Color online) (**a**) The dependences of α-spin and β-spin conductance (G) on the angle θ, respectively. (**b**) The spin filtering coefficient as a function of the angle θ. (**c**) The total conductance (G_s) as a function of the angle θ for Out-plane (square) and In-plane (circular), the data fitted well with Julliere's model (blue line). The inset shows the resistance difference of two cases as the function of the angle. (**d**) The anisotropic MR as a function of the angle θ.

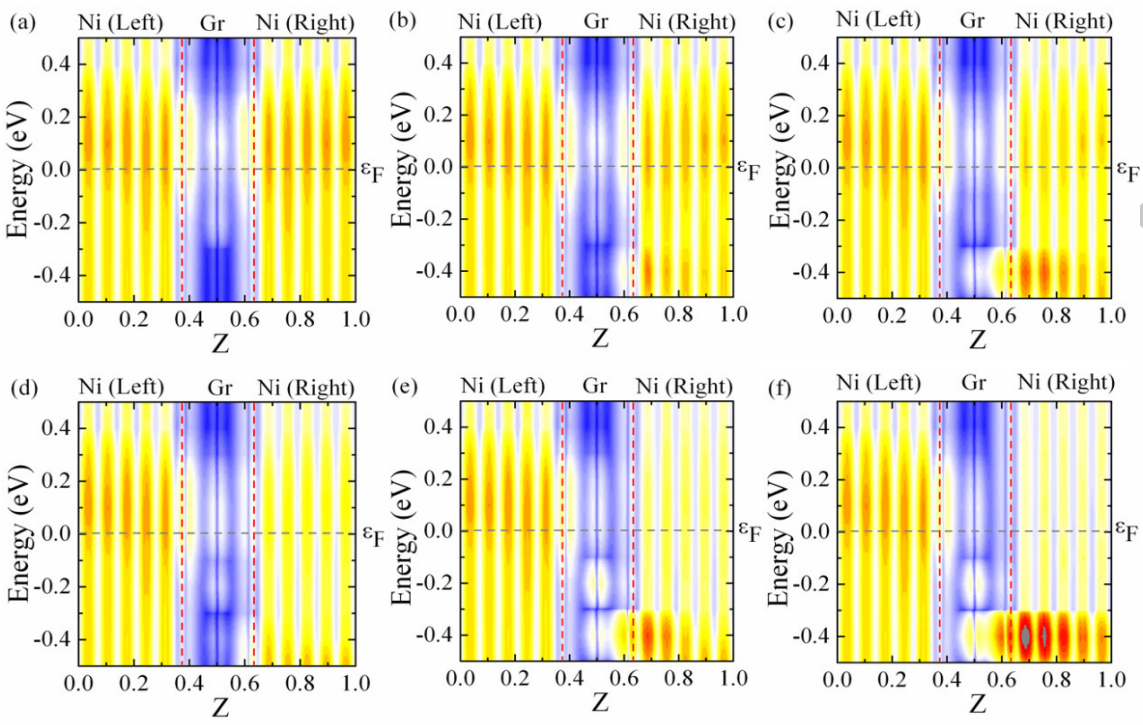

FIG. 4. (Color online) The local density of state of β-spin at different angles, from (**a**) to (**f**) the respective angle is 0°, 60°, 90°, 120°, 150°, 180°, respectively. The Fermi level is shifted to 0 (the gray dotted-line) and the red dotted-lines are a guide for the eye to the positions of Ni/Graphene (Gr) interface.

- Large TMR and spin filtering efficiency of Ni/graphene/Ni MTJ were theoretically investigated.
- The appropriate non-collinear magnetization calculation method has been introduced to systematically study the tunneling behavior of Ni/graphene/Ni MTJ with different magnetization directions.
- Theoretical research shows that the angle dependence of tunneling behavior originating from the resonant conduction states strongly affected by relative magnetization angle.